NOTATION

a = Peng-Robinson energy parameter
b = Peng-Robinson volume parameter
c = interfacial influence parameter
C = direct correlation function
f = Helmholtz free energy density
g = pair correlation function
k = Boltzmann's constant
n = number density
P = pressure
T = temperature
u = intermolecular potential
x = distance
y = mole fraction of species

Greek Letters

β = influence parameter scaling parameter
γ = surface tension
δ = adjustable energy parameter
∇ = gradient operator
ϵ = Lennard-Jones energy parameter
μ = chemical potential
σ = Lennard-Jones length parameter
ω = grand thermodynamic potential

Superscripts

0 = homogeneous fluid
+ = ideal fluid
* = dimensionless
I, II = bulk phases

Subscript

m = mixture

LITERATURE CITED

Benson, G. C., and V. T. Lam, "Surface Tensions of Binary Liquid Systems II. Mixtures of Alcohols," *J. Col. Int. Sci.*, **38**, 294 (1972).

Bongiorno, V., L. E. Scriven and H. T. Davis, "Molecular Theory of Fluid Interfaces," *ibid.*, **57**, 462 (1976).

Carey, B. S., L. E. Scriven and H. T. Davis, "Semi-Empirical Surface Tensions of Pure Normal Alkanes and Alcohols," *AIChE J.*, **24**, 1076 (1978).

Carey, B. S., "Molecular Thermodynamics of Multicomponent Interfaces," Ph.D. thesis, Univ. Minn., Minneapolis (1978).

Chu, J. C., S. L. Wang, S. L. Levy and R. Paul, *Vapor-Liquid Equilibrium Data*, J. W. Edwards, Ann Arbor, Mich. (1956).

Lam, V. T., and G. C. Benson, "Surface Tensions of Binary Liquid Systems. I. Mixtures of Non-electrolytes," *Can. J. Chem.*, **48**, 3774 (1970).

McCoy, B. F., and H. T. Davis, "On the Free Energy Theory of Inhomogeneous Fluids," *Phys. Rev.*, **A20**, 1201 (1978).

Peng, D. Y., and D. B. Robinson, "A New Two Constant Equation of State," *Ind. Eng. Chem. Fundamentals*, **15**, 59 (1976).

Vargas, A., Ph.D. thesis, "On the Molecular Theory of Dense Fluids and Fluid Interfaces," Univ. Minn., Minneapolis (1976).

Manuscript received August 30, 1978; revision received January 18 and accepted January 23, 1980.

Mass Transfer and Adsorption in Liquid Full and Trickle Beds

Experimental breakthrough curves were determined for a liquid full and a trickle bed reactor in which benzene was adsorbed from water on small activated carbon particles at 298°K and 1 atm. The step function of benzene was introduced into the water feed and the response measured in the liquid effluent. Benzene transfer also occurred from the liquid feed to the gaseous feed of pure helium.

Moment analysis of data for liquid full conditions indicated that the first moment of the response curve could be used to obtain the adsorption equilibrium constant K for benzene on activated carbon. Comparison of results obtained by this new method with the K value determined from static equilibrium runs demonstrated the validity of the moment theory.

Analysis of the response curves for trickle bed operation showed that the liquid-to-gas mass transfer coefficient $(ka)_L$ could be evaluated from either the zero or first moment. Results were obtained in both the trickling flow and pulse flow regimes. Values of $(ka)_L$ in the pulse flow regime, which were not heretofore available, were sharply higher than those for trickle flow.

HASSAN A. SEIRAFI
and
J. M. SMITH
University of California
Davis, California 95616

SCOPE

Mass transfer between gas and liquid and also between liquid and catalyst particles can significantly affect the performance of trickle bed reactors (Satterfield, 1978; Goto and Smith, 1975). Steady state methods have been used to obtain transport coefficients in the trickling flow (gas continuous) and pulsing flow regimes by steady state studies. These experiments have been carried out by two methods: in the absence of reaction by dissolution of solids which were unlike porous catalyst particles, or under catalytic reaction conditions where reaction effects have to be accounted for before mass transfer effects are evaluated.

One objective of our research was to use breakthrough curve (BTC) data to evaluate the gas-liquid mass transfer coefficient $(ka)_L$. Also, we wanted to carry out the experiments under conditions of rapid physical adsorption. Then equilibrium could be assumed at an intraparticle adsorption site, avoiding the complications of finite reaction rate and possible variations in catalyst activity, etc. The procedure was to measure breakthrough curves in the liquid effluent when a step function of

Hassan A. Seirafi is on leave from Abadan Institute of Technology, Abadan, Iran.

0001-1541-80-3778-0711-$00.95.

benzene in aqueous solution was passed through a bed of activated carbon particles. Some of this volatile adsorbate was adsorbed, but some also was transferred to the gas phase (feed of pure helium), and this permitted the determination of the mass transfer coefficient. For application of moment theory to the measured breakthrough curves, all transport processes in the trickle bed must be first order. This was achieved by using low concentrations (73 to 95 ppm) of benzene in the step input. The zero moment, which requires only the steady state end point of the breakthrough curve, is sufficient to determine one value of $(ka)_L$. A second value can be obtained from the first moment, which depends upon the entire breakthrough curve. Thus, the dynamic procedure permits one to compare two values of $(ka)_L$ obtained for the same flow conditions.

Little or no information appears to be available for $(ka)_L$ in the liquid flow rate range when the flow in a trickle bed reactor changes from the trickling to pulsing regime. A second objective was to extend the measurements into a higher liquid flow rate region so that the effect of changing regimes on $(ka)_L$ could be evaluated.

A further objective was to show that the adsorption equilibrium constant K could be obtained from dynamic experiments in liquid full beds packed with adsorbent particles. Hence, independent BTC were measured when benzene was introduced to the feed where water alone (no gas phase) flowed through a bed of carbon particles.

CONCLUSIONS AND SIGNIFICANCE

The data for benzene demonstrate that analysis of breakthrough curves for first-order systems can provide a reliable method for measuring liquid-to-gas mass transfer coefficients $(ka)_L$ in trickle beds. Results for the zero moment, which require only the final breakthrough concentration, are more accurate than $(ka)_L$ obtained from first moments of the BTC. In addition, the only equilibrium parameter necessary is the solubility of the adsorbing component in water (Henry's law constant). The sole rate constant involved in the first-moment expression also is $(ka)_L$, but the dynamic liquid holdup and the adsorption equilibrium constant are required as well.

Mass transfer coefficients were measured for small (0.077×10^{-2}m) particles as a function of liquid flow rate in a range that included the change from the gas continuous trickling regime to the pulsing regime. A sharp increase in $(ka)_L$ was observed at a liquid mass velocity between 10 and 12 kg/(m)^2(s). This is the flow rate where the change from trickling to pulsing flow has been observed (Weekman and Myers, 1964; Charpentier, 1976). In the trickling flow region, $(ka)_L$ was found to increase gradually with liquid rate, in agreement with available data. In the pulsing flow region, the increase was more rapid, and, in addition, our results were about 100% lower than those of Sato et al. (1972).

It was also demonstrated that the adsorption equilibrium constant K for benzene on activated carbon could be obtained from the first moment of breakthrough curves when the bed of particles was operated liquid full (no gas phase). The value of K determined in this way agreed well with the results of our independent measurements by the conventional static method for establishing the adsorption isotherm.

In principle, mass transfer coefficients $(ka)_s$ from liquid to particle can be evaluated by moment analysis of breakthrough curves but in practice this may be difficult. This is because mass transport between a flowing and stationary phase depends upon the second moment of the breakthrough curve. Such moments are difficult to evaluate accurately in trickle bed operation.

Interphase mass transfer can significantly retard the overall or global rate of reaction in trickle bed (con-current downflow) catalytic reactors (Satterfield, 1975; Gianetto et al; 1973; Goto and Smith, 1975). In such three-phase systems, both gas-to-liquid and liquid-to-catalyst mass transfer have been studied. A limited amount of experimental data has been obtained by steady state techniques for both types of transport. The resulting mass transfer coefficients have been correlated in terms of energy dissipation (pressure drop) (Reiss, 1967; Sylvester and Pitayagulsarn, 1976) or with flow geometry and physical properties (Sato et al., 1972).

The magnitude of mass transfer rates in trickle beds depends upon the nature of the gas and liquid flow. At low flow rates, a gas continuous, trickling liquid regime is observed. When either gas or liquid rate is increased, a more turbulent, pulsing region is evident (Weekman and Myers, 1964; Charpentier, 1976; Sato et al., 1973). The flow rate boundaries dividing these regimes are not sharp and not well correlated, as yet, in terms of the properties of the beds. Mass transfer results in the boundary regions are few. One of our objectives was to evaluate gas-to-liquid transfer coefficients $(ka)_L$ in the region dividing trickling and pulsing flow.

A second objective was to apply dynamic techniques to the measurement of $(ka)_L$. Such methods have been used (Schneider and Smith, 1968) to measure both equilibrium and rate parameters in two-phase (gas-solid) packed bed reactors. Also, dynamic methods have been employed in trickle beds (Columbo et al., 1976) to obtain contact or wetting efficiencies (fraction of the particle surface covered by liquid).

Our procedure was to measure the response (breakthrough curve) to a step input of tracer introduced into a bed of adsorbent particles. The water stream flowing through a bed of activated carbon particles was changed, at time zero, to water containing benzene. The benzene content of the liquid effluent was measured as a function of time to obtain the breakthrough curve (BTC). Two kinds of dynamic measurements were made. First, BTC were determined for upflow liquid full (no gas stream) operation of the bed. These data could be interpreted to give the adsorption equilibrium constant for the benzene-water and activated carbon system. Then the apparatus was operated as a trickle bed. Volatile benzene from the liquid feed was both absorbed and transferred to the gas (helium) stream. This distribution of benzene was a measure of the gas-to-liquid mass transfer, so that moments of the resulting BTC could be used to evaluate $(ka)_L$.

At low liquid rates in trickle beds, available data (Satterfield, 1975; Herskowitz et al., 1979) suggest that not all of the outer surface of the particles is covered by liquid. Also, for low tube-to-particle diameter ratios, the liquid may not be distributed uniformly across the bed diameter (Herskowitz and Smith, 1978). The design of the apparatus and the experimental conditions used in this study were chosen so as to avoid both of these conditions.

All data were obtained at 298°K and 1 atm pressure.

EXPERIMENTAL

For liquid full operation, the water flowed upwards through one of two Pyrex tubes containing a bed of activated carbon particles (20 to 24

TABLE 1. OPERATING CONDITIONS AND RESULTS FOR LIQUID FULL RUNS

Temperature 25°C, pressure 1 atm, particle size 7.7×10^{-4} m, mesh size range 20-24

	Run A_2	Run A_3	Run A_4	Run A_5	Run A_6
Reactor ID $\times 10^2$, m	1.08	1.08	1.57	1.08	1.08
Mass of carbon $\times 10^3$, kg	1.85	1.35	2.40	1.85	1.85
Length of carbon packing $\times 10^2$, m	4.1	3.0	2.4	4.1	4.1
Bed void fraction	0.507	0.509	0.494	0.507	0.507
Liquid superficial velocity $\times 10^2$, m/s	6.6	4.6	10.6	8.6	10.7
First absolute moment, s	979	957	338	656	574
Benzene conc. in step-function input, ppm	83	93	82	84	88

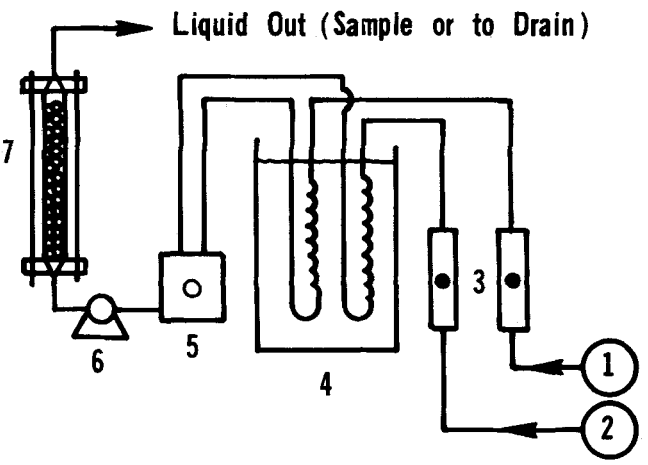

Figure 1. Schematic diagram of apparatus for liquid-full operation. 1, solution feed; 2, water feed; 3, rotameters; 4, constant temperature bath; 5, 3-way valve; 6, pump; 7, reactor.

mesh). Dimensions of the beds and particles are given in Table 1, and the apparatus is shown in Figure 1. The particles were held in place with stainless steel screens. The flow was changed from deionized water to an aqueous solution, containing 85 to 95 ppm of benzene, with a three-way valve. Samples were withdrawn from the liquid effluent, at intervals ranging from 1 to 25 min, for analysis.

In trickle bed operation (see Table 2 and Figure 2), the liquid was distributed through a movable, Plexiglas cylinder equipped with an O ring to hold the distributor tightly against the Pyrex tube. The liquid flowed from a cylindrical distributor to the top of the bed through twelve stainless steel capillary tubes (0.1×10^{-2} m ID and 0.5×10^{-2} m long) located in the bottom circular plate of the Plexiglas cylinder. The twelve tubes were located so as to give essentially uniform liquid distribution to the top of the bed. The lower ends of the capillaries extended to within about 5×10^{-4} m of the bed of particles. The gas was fed to the center of the Pyrex tubing through a 0.32×10^{-2} m tube passing through the center of the Plexiglas distributor. Below the bottom screen holding the particles was a 6×10^{-2} m long section of the Pyrex tube, designed to serve as a separator for gas and liquid. The gas was removed via a 0.32 m ID stainless steel tube inserted vertically in this section, as shown in Figure 2. The open end of the tube was shielded from liquid by a stainless steel cap. The liquid was withdrawn from the bottom of the Pyrex tube at a rate such that a nearly constant liquid level was maintained in the separator. Samples were taken from this outlet for analysis.

The breakthrough time was of the order of hours (Figure 4), while the average residence time of the liquid in the separator was 5 to 10 s. Hence, the retention time and dispersion of the liquid in the separator did not have a significant effect on the measurement of the breakthrough curve. The dead volume of liquid between the three-way valve and the bed and between the bed effluent and the sample point was made as small as possible. However, its magnitude was also not important because of the relatively short residence time in these volumes. Mass transfer in the separator was significant and had to be accounted for as described in the results section.

Type BPL activated carbon was used. This material has a surface area of about $1.10 \times 10^6 m^2/kg$, particle density of 800 kg/m^3, and porosity of 0.60 (Bulletin 23-106A, 1974). Prior to use the carbon was sieved, washed to remove adhering fines and then dried at 110°C until the weight was constant. Before each run, the carbon charge was boiled for ½ hr in distilled water to fill the pores with liquid. The carbon beds were packed by first filling the Pyrex tube with water and then adding the particles. Deionized water was employed for both liquid full and trickle bed runs. Helium (stated purity = 99.99%) was used for the gas stream in the trickle bed runs.

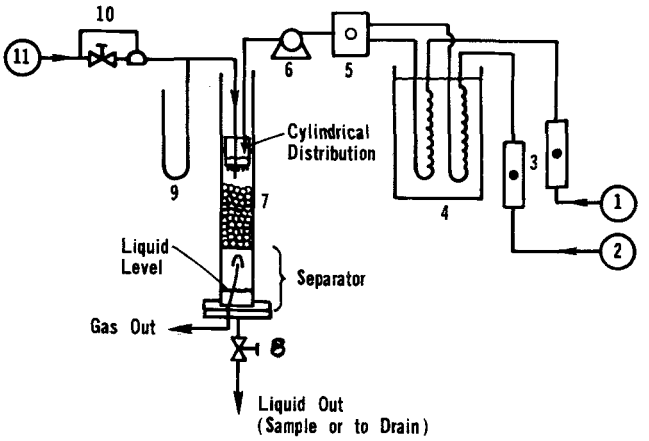

Figure 2. Schematic diagram of apparatus for trickle-bed operation. 1, solution feed; 2, water feed; 3, rotameters; 4, constant temperature bath; 5, 3-way valve; 6, pump; 7, reactor; 8, needle valve; 9, manometer; 10, flow regulator; 11, helium cylinder.

TABLE 2. OPERATING CONDITIONS AND RESULTS FOR TRICKLE BED RUNS

Temperature 25°C
Particle size = 0.108×10^{-2} m
(Mesh size range 16-18)

Pressure 1 atm
Gas superficial velocity = 6.74×10^{-2} m/s
Mass of carbon = 3.5×10^{-3} kg

Reactor ID = 1.58×10^{-2} m
Bed void fraction = 0.575
Bed length = 4.2×10^{-2} m

			Zero moment		First moment	
Run #	C_0, ppm	$u_L \times 10^2$, m/s	$(m_0)^*_L = \frac{(C_L)_{t=\infty}}{C_0}$	$(ka)_L$, s^{-1}	$(u_1)_L$, s	$(ka)_L$, s^{-1}
5	75	1.25	0.847	0.054	4 240	0.072
6	90	1.22	0.852	0.050	4 350	0.055
7	88	1.57	0.853	0.066	3 370	0.089
8	86	1.17	0.838	0.053	4 540	0.060
9	75	0.90	0.897	0.024	5 940	0.024
10	74	0.64	0.887	0.019	8 350	0.024
11	82	0.36	0.859	0.013	14 800	0.020
12	73	1.00	0.895	0.028	5 350	0.036
13	94	1.01	0.903	0.025	5 290	0.031
14	82	0.51	0.864	0.018	10 600	0.025

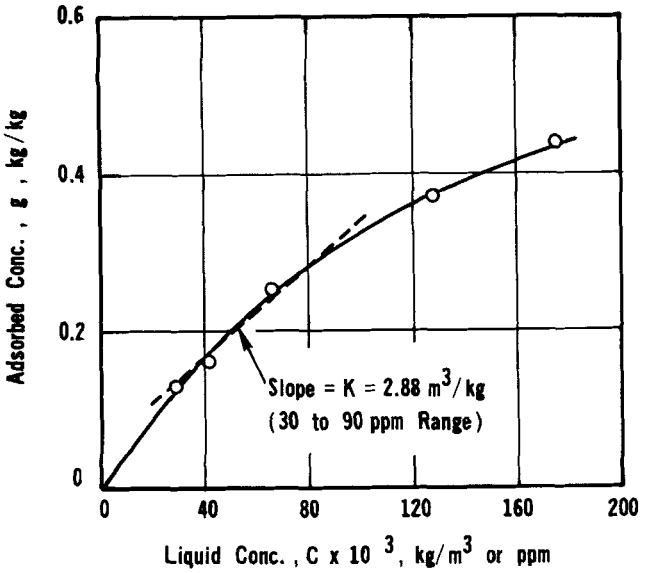

Figure 3. Equilibrium adsorption isotherm for benzene on carbon at 298K (static method).

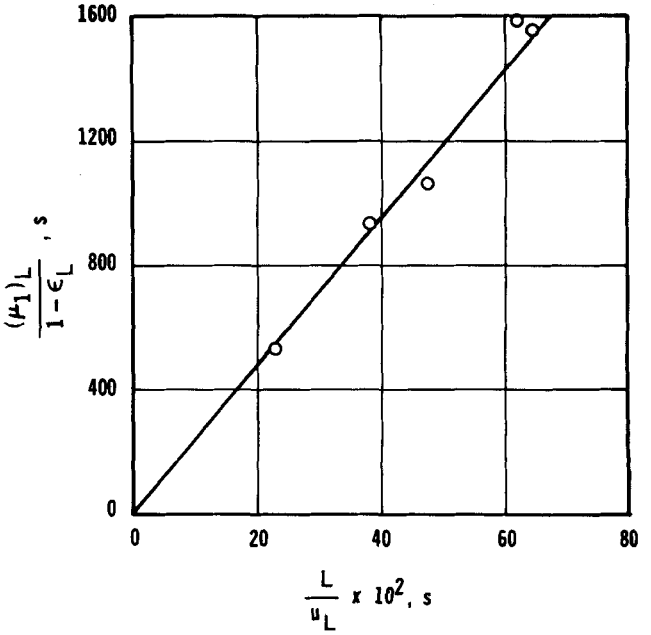

Figure. 4. First-moment function for liquid-full operation.

The benzene concentration in the liquid samples was determined in a gas chromatograph (flame-ionization detector) with a Porapak-Q column 0.60 m long and operated at 423°K. Calibration runs indicated that the peak height was directly proportional to the benzene concentration up to at least 120 ppm.

As a test of the dynamic runs, the adsorption equilibrium was also measured by static experiments. Measured amounts of activated carbon particles ($d_p = 0.077 \times 10^{-2}$m) were added to benzene-water solutions containing known amounts of benzene. Concentrations in the liquid were measured after the slurries were stirred for 96 hr. Additional determinations 24 hr later were unchanged within the sensitivity of the data.

The liquid flow rate was measured by collecting the water for a known time period, and the gas rate was measured with a soap-film meter and maintained constant with a Moore flow regulator (see Figure 2).

In preliminary runs the upstream pressure increased continually with time until, finally, the column flooded. A greenish layer of material was found to be depositing on the carbon particles. This problem was eliminated by adding Cu SO_4 to the deionized water to give a concentration of Cu^{++} of 2 to 3 ppm. The water was then filtered through an auxiliary bed of activated carbon, before the benzene was added, to prepare the feed for the runs.

THEORY

For our system of slightly soluble benzene, the gas-to-liquid mass transfer coefficient is controlled by the resistance in the liquid film. Then, the liquid phase concentration at the gas-liquid interface is that in equilibrium with the bulk gas value. Since Henry's law is valid for benzene in water at low concentrations and 298°K, the interface concentration is $C = C_g/H$, where $H = 0.20$ (Misic and Smith, 1971). Also, the physical adsorption of benzene on activated carbon is intrinsically rapid. Then the adsorbed concentration q is essentially in equilibrium with that in the liquid at the same radial position (r) in the particle; that is, q and C are related by the adsorption isotherm. At low concentrations, the isotherm is nearly linear over a range of liquid concentrations, so that

$$dq = KdC_i \tag{1}$$

With these restraints, and for plug flow of gas and of liquid in the trickle bed, mass conservation equations for gas, bulk liquid and intraparticle liquid are

$$u_g \frac{\partial C_g}{\partial x} + \epsilon_g \frac{\partial C_g}{\partial t} + (ka)_L\left(\frac{C_g}{H} - C\right) = 0 \tag{2}$$

$$u_L \frac{\partial C}{\partial x} + \epsilon_L \frac{\partial C}{\partial t} + (ka)_s[C - (C_i)_{r=R}] - (ka)_L\left(\frac{C_g}{H} - C\right) = 0 \tag{3}$$

$$D_e\left(\frac{\partial^2 C_i}{\partial r^2} + \frac{2}{r}\frac{\partial C_i}{\partial r}\right) - \epsilon_s \frac{\partial C_i}{\partial t} + \rho_p\left(\frac{\partial q}{\partial t}\right) = 0 \tag{4}$$

Boundary and initial conditions for a concentration input $C_0(t)$ in the liquid feed are

at $r = 0$

$$\frac{\partial C_i}{\partial r} = 0 \tag{5}$$

at $r = R$

$$D_e\left(\frac{\partial C_i}{\partial r}\right)_{r=R} = k_s[C - (C_i)_{r=R}] \tag{6}$$

at $t = 0$

$$C_g = C = C_i = q = 0 \text{ for all } x \tag{7}$$

at $x = 0$

$$C_{g0}(t) = 0 \tag{8}$$

at $x = 0$

$$C_0 = C_0(t) \tag{9}$$

This set of linear differential equations can be solved in the Laplace domain and the result, $\bar{C}(s, x)$, evaluated at the end of the bed to give $\bar{C}(s, L)$. Then, the dimensionless moments $(m_n)^*_L$ of the response curve $C(t, L)$ in the real time domain are obtained from

$$(m_n)^*_L = (-1)^n \lim_{s\to 0}\left[\frac{d^n \bar{\theta}_L(s,1)}{ds^n}\right] \tag{10}$$

where $\bar{\theta}_L$ is a dimensionless concentration related to $\bar{C}_L$ by the definition $\bar{\theta}_L = \bar{C}_L/\bar{C}_0$. Equation (10) provides explicit, theoretical equations for the moments in terms of the equilibrium and rate parameters of the system described by Equations (1) to (9)

In terms of dimensionless parameters, experimental values of the moments can be obtained from the measured BTC with the equation

$$(m_n)^*_L = \int_0^\infty \theta_L(\tau, 1)\, \tau^n\, d\tau \tag{11}$$

$$\tau = tu_L/L\epsilon_L$$

By equating the experimental moments determined from Equation (11) to the corresponding theoretical moment expression from Equation (10), equilibrium and rate parameters can be evaluated. This is the procedure used to obtain the results given in the remainder of the paper.

Test data indicate that only zero and first moments can be accurately measured in trickle beds. Ramachandran and Smith (1979) have obtained solutions of Equation (10) for these two moments. For a pulse (Dirac-Delta function) input, their results for $(m_0)^*_L$ and $(m_1)^*_L$ reduce to

$$(m_0)^*_L = \frac{1}{1+\beta}\{\beta \exp[-\alpha(1+\beta)] + 1\} \tag{12}$$

$$(m_1)^*_L = \frac{(m_0)^*_L (1-\beta)(\omega+\delta)}{\alpha(1+\beta)^2} + \frac{1}{\alpha(1+\beta)^2}\{[\beta(\delta+\omega) - \alpha\beta(\beta\delta - \omega)] \exp[-\alpha(1+\beta)] - [\delta + \omega - \alpha(\beta\omega - \delta)]\} \tag{13}$$

For the special case of liquid full operation ($u_g = 0$), these expressions simplify to

$$(m_0)^*_L = 1 \tag{14}$$

$$(m_1)^*_L = 1 + \frac{\alpha_s\gamma(\epsilon_s + K^*)}{3(Sh)} \tag{15}$$

In our experience it was more accurate to use a step input than a pulse input. Hence, it is necessary to calculate experimental values of the moments from the breakthrough curves. Following Ammons et al. (1977), the required equation for liquid full operation is (only the first moment is useful since the zero moment is unity for a reversible process)

$$(\mu_1)_L = \frac{1}{C_0}\int_0^\infty (C_0 - C_L)\,dt \tag{16}$$

The expression for $(\mu_1)_L$ in terms of the dimensionless moments is

$$(\mu_1)_L = \frac{(m_1)^*_L}{(m_0)^*_L}\left(\frac{L\epsilon_L}{u_L}\right) \tag{17}$$

If we use Equations (14) and (15) in (17), the theoretical expression for the first absolute moment for liquid full operation is

$$(\mu_1)_L = \frac{L}{u_L}(1-\epsilon_L)\rho_p K \tag{18}$$

In this equation, accumulation terms in the liquid phase have been neglected with respect to the adsorption accumulation term (these neglected terms are less than 0.1% of the total).

For trickle bed operation, both moments are useful. The equations for obtaining moments from the experimental BTC are

$$(m_0)^*_L = \frac{(C_L)_{t=\infty}}{C_0} \tag{19}$$

where $(C_L)_{t=\infty}$ is the steady state value attained at the end of the BTC, and

$$(\mu_1)_L = \frac{1}{(C_L)_{t=\infty}}\int_0^\infty [(C_L)_{t=\infty} - C_L]\,dt \tag{20}$$

The theoretical expressions for $(m_0)^*_L$ and $(\mu_1)_L$ are Equations (12) and (17), with $(m_1)^*_L$ given by Equation (13).

RESULTS

Adsorption Equilibrium Constant (Liquid Full Data)

Figure 3 shows the adsorption isotherm determined by static measurements. In the range of concentrations employed in the dynamic experiments ($30 < C < 95$ ppm), the data closely follow a straight line with a slope of $K = 2.88$ m^3/kg. It is not necessary that the isotherm go through the origin in order to apply the moment theory culminating in Equations (12) and (13). It is sufficient if the slope of the equilibrium relation is constant over the range of concentrations used in the experiments.

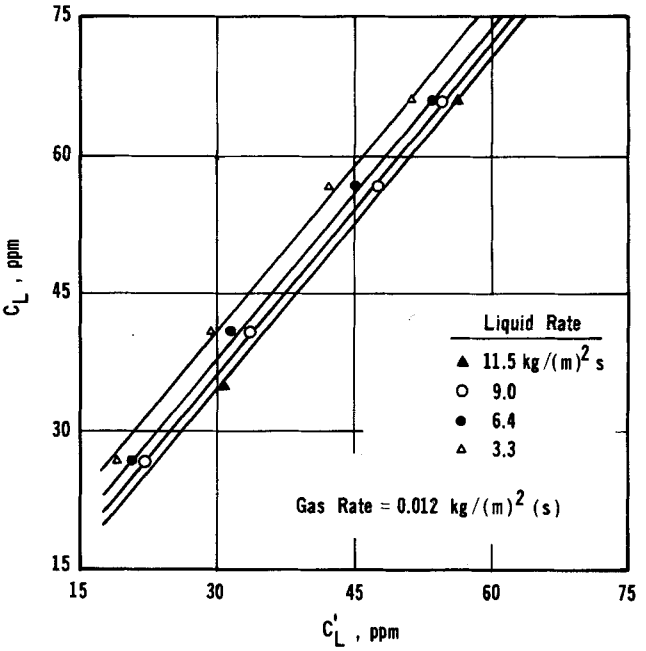

Figure 5. Relation between concentration C'_L, in reactor effluent, and C_L at bottom of packing.

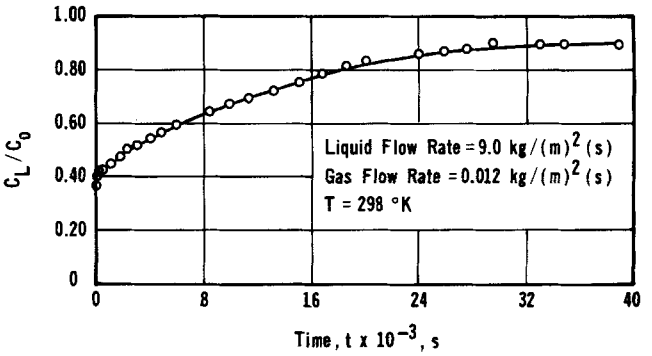

Figure 6. Typical breakthrough curve for trickle-bed operation.

Equation (18) indicates that K also can be determined from the first absolute moment, the liquid superficial velocity u_L and the properties of the bed. Figure 4 is a graph of such information for the liquid full runs, where $(\mu_1)_L$ was evaluated from the BTC using Equation (16). The data establish a reasonably well-defined straight line whose slope, according to Equation (18), is equal to $\rho_p K$. This slope gives $K = 3.00$ m^3/kg. The good agreement between the values evaluated by the static and dynamic methods lends confidence to the accuracy of the experimental BTC and the adequacy of the moment theory. In calculating $(\mu_1)_L$ from Equation (16), a polynomial which gave the best fit to the experimental points was used. It is concluded that the adsorption equilibrium constant can be accurately determined from dynamic data obtained in a liquid full, packed bed of adsorbent particles.

Gas-To-Liquid Mass Transfer Coefficient (Trickle Bed Data)

The experimental zero and first moments obtained from Equations (19) and (20) depend upon the liquid phase concentration (C_L) at the bottom of the bed. However, the liquid can only be sampled for analysis in the exit stream from the separator (Figure 2). Hence, a correction must be made for the extent of

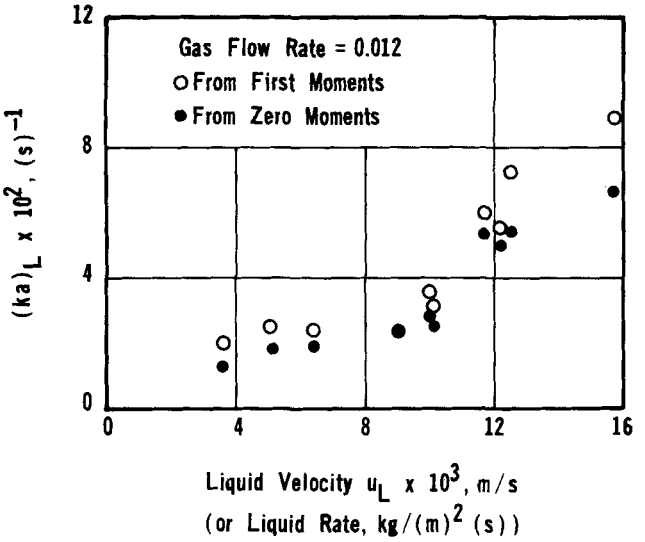

Figure 7. Liquid-to-gas mass transfer coefficients from zero and first moments.

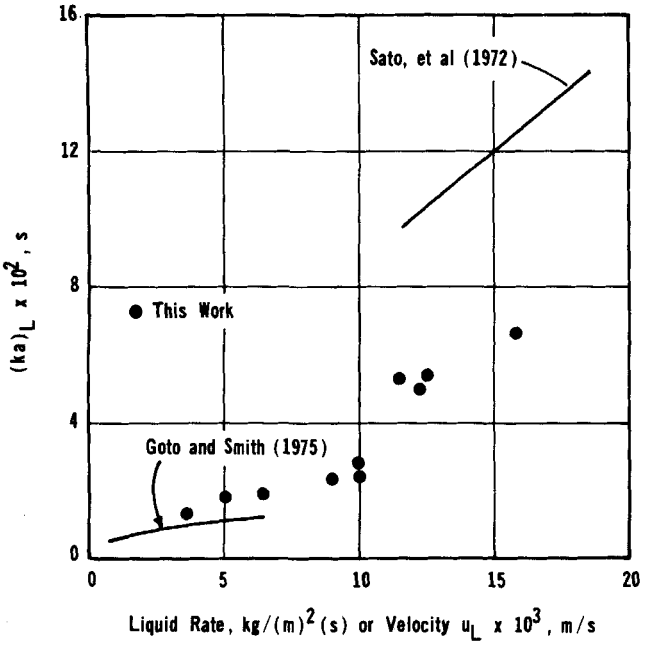

Figure 8. Effect of liquid rate on liquid-to-gas mass transfer coefficient.

mass transfer in the separator. Such corrections will depend upon the liquid and gas rates and the liquid level in the separator and, of course, would be necessary for steady state as well as dynamic methods. The liquid level determines the volume of gas through which the liquid drops fall and in which mass transfer occurs. This liquid level was maintained the same in all the experiments by adjusting the needle valve in the effluent liquid stream. It was considered most accurate to make the correction experimentally. The concentration in the effluent liquid C_L' was measured when the bed was eliminated, and the liquid distributor was placed just above the bottom screen which normally held the particles. The difference between the feed concentration (C_L) and C_L' obtained in these blank runs is a measure of the mass transfer in the separator. The results are shown in Figure 5 as a plot of C_L vs. C_L' for various liquid flow rates. This graph was used for the trickle bed runs to obtain C_L from the measured C_L'.

A typical BTC is illustrated in Figure 6. Experimental values of m_0^* and $(\mu_1)_L$ were evaluated from such BTC using Equations (19) and (20). The results are given in Table 2. The zero moment is independent of the curve itself and depends only on the steady state concentration in the effluent.

The mass transfer coefficient $(ka)_L$ can be calculated from either $(m_0^*)_L$ or $(\mu_1)_L$. In using the zero moment data, α is first calculated from Equation (12), after β is evaluated from the liquid and gas flow rates and the Henry law constant. As mentioned, H was taken as 0.20 at 25°C (Misic and Smith, 1971). However, the value of α is not very sensitive to H; a 60% change in the Henry law constant causes an 8% change in $(ka)_L$. The mass transfer coefficient in terms of α is

$$(ka)_L = \alpha \frac{Hu_g}{L} \tag{21}$$

The coefficients determined in this way from the zero moment data are shown as a function of liquid flow rate in Figure 7. It should be noted that these results, while obtained from the zero moment, are identical to those obtained from a steady state equation for $(ka)_L$. No dynamic information is needed but only the steady state concentration attained at the end of the BTC.

When the definitions of the dimensionless parameters are substituted in Equations (12) and (13) to obtain $(m_0)_L^*$ and $(m_1)_L^*$, the first moment expression [Equation (17)] is found to be independent of all rate parameters except $(ka)_L$. However, $(\mu_1)_L$ is a function of K and of the dynamic liquid holdup ϵ_L. We know the adsorption equilibrium constant from the liquid full data, and ϵ_L can be estimated from the dimensional correlation of Satterfield and Way (1972):

$$\epsilon_L = A_1(u_L)^{1/3}(\mu)^{1/4} \tag{22}$$

Goto and Smith (1975) found Equation (22) to correlate satisfactorily their holdup data for particle diameters less than 0.3×10^{-2} m. For the particle size used in our work, A_1 is estimated to be 7.17, when SI units are used for the liquid velocity and holdup. With K and ϵ_L known, Equation (17) can be solved numerically for $(ka)_L$. The results, and the moment values, are shown in Table 2 and in Figure 7. In Equation (17), $(ka)_L$ is insensitive to variations in ϵ_L but very sensitive to changes in K.

The two sets of mass transfer coefficients agree reasonably well, although the values from the first moment scatter more, average about 35% higher and exhibit a less well-defined trend with liquid flow rate. Since the zero moment calculations do not involve K or ϵ_L and depend only on the final steady state effluent concentration, they are believed to be more accurate.

DISCUSSION OF PULSING FLOW RESULTS

The mass transfer coefficients in Figure 7 increase abruptly at a liquid mass velocity between 10 and 12 kg/(m)^2(s). Both Weekman and Myers (1964) and Charpentier (1976) in flow regime studies found that there is a change from trickling to pulsing liquid flow at about 12 kg/(m)^2(s). Visual observation of the flow in our Pyrex tube indicated that pulsing began at about 10 to 11 kg/(m)^2(s). It is concluded that the apparent discontinuity in the results for $(ka)_L$ as the liquid rate increases is due to the initiation of pulsing flow. Sato et al. (1973) did not observe the change in flow regime until a higher liquid rate. However, the transition probably depends upon particle size and properties of the liquid and gas. Much larger particles were employed by Sato and colleagues than were used in our study.

The discontinuity in $(ka)_L$ can be seen more clearly in Figure 8, where only the more accurate results obtained from the zero moment data are plotted. In the trickling flow regime, the correlation of Goto and Smith (1975) is applicable and is shown in Figure 8 as the lower curve. The agreement of this correlation with our data is reasonably good over the liquid rate range covered by Goto and Smith, but the deviation increases as the change in flow regime is approached.

Most available correlations in the pulsing regime are based upon the energy dissipation rate which was not measured in our work. The only correlation which can be used for comparison is that of Sato et al. (1972), which is represented by the upper straight line in Figure 8. This line gives coefficients about twice as large as those obtained from our data. The Sato correlation does not include the physical properties of the system, since

$(ka)_L$ is given as the dimensional equation

$$(ka)_L = 0.980(d_p)^{-0.5}(u_L u_g)^{0.8} \quad (23)$$

This could be one explanation for the large deviation in Figure 8. However, the nature and extent of pulsing flow would seem to depend upon the characteristics of the individual system (perhaps such factors as the tube diameter, particle shape and type, liquid distribution, etc.) which are not accounted for in Equation (23). Also, there may be some question about the validity of the plug flow assumption [Equations (2) and (3)] in the pulsing regime.

ACKNOWLEDGMENT

This research was carried out with the financial assistance of National Science Foundation Grant ENG 77-10166 and NATO Grant 1474. Constructive discussions with Professor A. Gianetto, Polytechnic Institute of Turin, Italy, are gratefully acknowledged. The Calgon Corporation provided the activated carbon.

NOTATION

A_1 = dimensional coefficient defined by Equation (22)
C_g = concentration of adsorbate (benzene) in the gas, kmole/m^3
$C_{g0}(t)$ = disturbance function for concentration of adsorbate in the gas feed stream, kmole/m^3
C_i = concentration of adsorbate in the pores of the particles, kmole/m^3
C = concentration of adsorbate in the liquid, kmole/m^3
$C_0(t)$ = disturbance function for concentration of adsorbate in the liquid feed stream, kmole/m^3
C_0 = step concentration of adsorbate in liquid, kmole/m^3
C_L = adsorbate concentration in liquid at exit of bed, kmole/m^3
$(C_L)_{t=\infty}$ = steady state concentration of adsorbate in the liquid at the exit of bed, kmole/m^3
C'_L = concentration of adsorbate in the liquid at the exit of the separator (see Figure 2), kmole/m^3
D_e = effective diffusivity of adsorbate in the liquid in the pores of the particles, m^2/s
d_p = particle diameter, m
H = Henry's law constant, [mole/(m^3 of gas)]/(mole/m^3 of liquid)]
k_s = liquid particle mass transfer coefficient, m/s
$(ka)_L$ = volumetric gas-liquid mass transfer coefficient, s^{-1}
$(ka)_s$ = volumetric liquid particle mass transfer coefficient, s^{-1}
K = adsorption equilibrium constant, m^3/kg
K^* = $K\,\rho_p$
$(m_n)^*_L$ = dimensionless nth moment, defined by Equation (10)
L = length of packed bed, m
q = surface (adsorbed) concentration of adsorbate, kmole/kg
r = radial distance from center of the catalyst particle, m
R = radius of the catalyst particle, m
s = Laplace transform variable
Sh = modified Sherwood number, $k_s R/D_e$
t = time, s
u_g = superficial gas velocity, m/s
u_L = superficial liquid velocity, m/s
x = axial distance from entrance to packed bed, m

Greek Letters

α = dimensionless gas-liquid mass transfer coefficient, $\alpha = (ka)_L L/Hu_g$
α_s = dimensionless solid-liquid mass transfer coefficient, $\alpha_s = (ka)_s L/u_L$
β = $u_g H/u_L$
γ = $R^2 u_L/D_e L\epsilon_L$
δ = $-[1 + \alpha_s\gamma(\epsilon_s + K^*)/3\,Sh]$
ϵ_g = gas holdup volume divided by volume of empty column
ϵ_L = dynamic external liquid holdup volume divided by volume of empty column
ϵ_s = porosity of the catalyst particle
θ_L = C_L/C_0
ρ_p = particle density, kg/m^3
τ = $t\,u_L/L\epsilon_L$
ω = $\epsilon_g u_L/\epsilon_L u_g$
μ = liquid viscosity, kg/(m)(s)
$(\mu_1)_L$ = first absolute moment of the response in the liquid, s

LITERATURE CITED

Ammons, R. D., N. A. Dougharty and J. M. Smith, "Adsorption at Methylmercuric Chloride on Activated Carbon. Rate and Equilibrium Data," *Ind. Eng. Chem. Fundamentals*, **16**, 263 (1977).

Charpentier, J. C., "Recent Progress in Two Phase Gas-Liquid Mass Transfer in Packed Beds," *The Chem. Eng. J.*, **11**, 161 (1976).

Colombo, A. J., G. Baldi and S. Sicardi, "Solid-Liquid Contacting Effectiveness in Trickle Bed Reactors," *Chem. Eng. Sci.*, **31**, 1101 (1976).

Gianetto, A., V. Specchia and G. Baldi, "Absorption in Packed Towers with Concurrent Downward High-Velocity Flows. II: Mass Transfer," *AIChE J.*, **19**, 916 (1973).

Goto, S. and J. M. Smith, "Trickle-Bed Reactor Performance Part I. Holdup and Mass Transfer Effects," *ibid.*, **21**, 706 (1975).

Herskowitz, M., and J. M. Smith, "Liquid Distribution in Trickle-Bed Reactors. Part I. Flow Measurements," *ibid.*, **24**, 439 (1978).

Herskowitz, M., R. Carbonell and J. M. Smith, "Effectiveness Factors and Mass Transfer in Trickle Reactors," *ibid.*, **25**, 272 (1979).

Misic, D. M., and J. M. Smith, "Adsorption of Benzene in Carbon Slurries," *Ind. Eng. Chem. Fundamentals*, **10**, 381 (1971).

Ramachandran, P. A., and J. M. Smith, "Dynamic Behavior of Trickle-Bed Reactors," *Chem. Eng. Sci.*, **34**, 75 (1979).

Reiss, L. P., "Cocurrent Gas-Liquid Contacting in Packed Columns," *Ind. Eng. Chem. Process Design Develop.*, **6**, 486 (1967).

Sato, Y., T. Hirose, F. Takahashi and M. Toda, "Performance of Fixed-Bed Catalytic Reactor with Co-current Gas-Liquid Flow," *Pacific Chem. Eng. Cong.*, Sec. 8, 187 (1972).

Sato, Y., and Y. Hashiguchi, "Flow Pattern and Pulsation Properties of Cocurrent Gas-Liquid Downflow in Packed Beds," *J. Chem. Eng. Japan*, **6**, 315 (1973).

Satterfield, C. N., and P. F. Way, "The Role of the Liquid Phase in the Performance of a Trickle Bed Reactor," *AIChE J.*, **18**, 305 (1972).

Satterfield, C. N., "Trickle-Bed Reactors," *ibid.*, **21**, 209 (1975).

———, M. W. Van Eek and G. S. Bliss, "Liquid-Solid Mass Transfer in Packed Beds with Downward Concurrent Gas-Liquid Flow," *ibid.*, **24**, 709 (1978).

Schneider, P., and J. M. Smith, "Adsorption Rate Constants from Chromatography," *ibid.*, **14**, 762 (1968).

Sylvester, N. D., and P. Pitayagulsarn, *Ind. Eng. Chem. Process Design Develop.*, **14**, 421 (1975); *ibid.*, **15**, 360 (1976).

Weekman, V. W., Jr., and J. E. Myers, "Fluid-Flow Characteristics at Concurrent Gas-Liquid Flow in Packed Beds," *AIChE J.*, **10**, 951 (1964).

Manuscript received June 28, 1979; revision received November 26, and accepted December 21, 1979.